# Setup of a Simulation Based Forecast of Critical Quality Metrics for Thermoplastic Automated Fiber Placement

Lars BRANDT, Fanny RICLET, Dominik DEDEN and Frederic FISCHER
Center for Lightweight Production Technology,
German Aerospace Center (DLR)
Am Technologiezentrum 4
86159 Augsburg

## ABSTRACT

Climate change is posing a challenge on the aeronautic industry to reduce and decarbonize commercial aviation. In this light new airplane concepts are created and vigorously developed. Whereas current CFRP fuselages use thermoset materials decision has not yet been made for zero emission aircrafts. In this context carbon fiber reinforced thermoplastics polymers (CFRPs) offer distinct advantages in their mechanical and thermal properties. For example, their high resistance under typical aircrafts use temperatures conditions, short curing cycles, weldability and recyclability. These render the material an interesting choice for new airplanes. Thermoplastic Automated Fiber Placement (TP-AFP) is a promising manufacturing process for the material due to its high automatization and the ability to quickly produce complex shaped structures. In case of in situ consolidation, the quality of the final part is determined during the layup. Thus, optimization of processing parameters is essential.
For this reason, this study aims to forecast the quality metrics for laminates produced by TP-AFP. A model is presented that predicts the evolution of crystallization and bonding quality of the carbon fiber reinforced, low melt PAEK (CF/LM-PAEK). The temperature history is obtained via an existing heat transfer simulation and fed into the proposed model to predict quality metrics. Prediction accuracy is shown via mechanical characterization of laminates and shows good correlation.

## 1. INTRODUCTION

Carbon fiber reinforced polymers are particularly interesting in the aeronautics and aerospace industries. These materials allow to reduce weight which is a key challenge in the context of climate change as less energy is required over the entire life cycle. Thermosets have been largely used for a variety of aeronautic applications in the past. However, thermoplastic polymers are even more promising matrices as they can be molten. This offers opportunities for recyclability, repair and weldability, which facilitate their integration in complex and large structures.

Automated Fiber Placement of reinforced thermoplastics is an additive production process that makes use of the inherent advantages of a thermoplastic matrix system for CFRPs. Even more so if in-situ consolidation renders additional process steps such as autoclaves unnecessary. A current challenge for this process is to eliminate knock-down factors due to insufficient consolidation. One solution is to optimize processing parameters. However this involves optimizing interrelated parameters that directly influence material final characteristics, like the roller pressure on the tape, the temperature gradient created by the laser heat source or the velocity of the placement head. Furthermore, each introduction of new materials, needs the identification of the adjusted process parameters. In this study CF/LM-PAEK, a semi-crystalline thermoplastic which can be melted at lower temperatures than other polyaryl ether

ketone polymers, is used. A concept is presented to avoid laborious trials to identify the optimum process parameters by developing a simulation that uses the process parameters (laser power, velocity of the roller) and the material characteristics as inputs and quantifies the quality of the AFP-manufactured part.

For this, existing models for bonding and crystallization are identified and adapted for TP-AFP and CF/LM-PAEK. Subsequently an existing finite element simulation developed at the DLR is used to predict temperature gradients in the composite tapes from the process parameters It is used as input for the developed quality prediction model. The models are validated via AFP trials and the limitation and requirements to fit them on the transient process will be outlined.

## 2. DESCRIPTION OF THE TP-AFP PROCESS

The Automated Fiber Placement often uses a gantry or robot arm equipped with a placement head to lay down prepreg tapes. A diagram of this process is presented in Figure 1. The laminate is built up layer by layer placing new tapes on top of already placed substrate. Tape is fed to a consolidation roller where the laminate and tape are heated above melting temperature. For in situ consolidation to occur intimate contact between the bonding partners has to be established. Key factors for the degree of intimate contact are material viscosity, surface roughness and applied pressure. Afterwards polymer chains of the matrix can migrate at the interface and will form a homogeneous material.

The AFP process conditions should be chosen to maximize the consolidation which results in processing temperatures near to thermal degradation. However, the cooling rate between melt and glass transition temperature of the thermoplastic resin defines its final crystallization rate, important for its mechanical characteristics. In general, lower cooling rates result in higher crystallinity which contradicts with the goal of high depositioning rates needed in the industry. Therefore, a sufficient crystallinity has to be defined and met by the process.

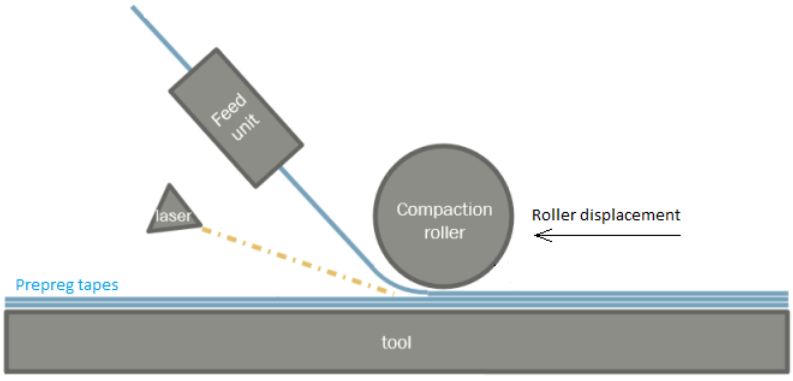


*Figure 1: Automated fiber placement with in situ consolidation*

## 3. QUALITY PREDICTION MODELS

As laid out, bonding and the crystallization are key factors to assess the quality of the CFRP component produced by TP-AFP. Both have a strong influence on the final mechanical characteristics of parts. In this section, the physical effects are explained in detail, existing models used to describe the bonding and crystallization kinetics are presented and adapted to the material and process.

## 3.1 Bonding Models

### *3.1.1 State of the art and model selection*

One of the advantages of thermoplastics polymers is their ability to be consolidated in situ. The different layers are bonded together during the placement of the tapes, thanks to the heat and pressure applied. This process will therefore depend on the pressure applied by the roller, the temperature produced by the laser source, the dwell time or exposure time as well as the cooling rate.

In literature in-situ consolidation is described in two steps: the closure of the voids at the interface and the migration of the polymer chains between the two layers, which create a strong bonding. This description leads to two models, in which the temperature and pressure histories are coupled: the intimate contact model and the self-autohesion model.

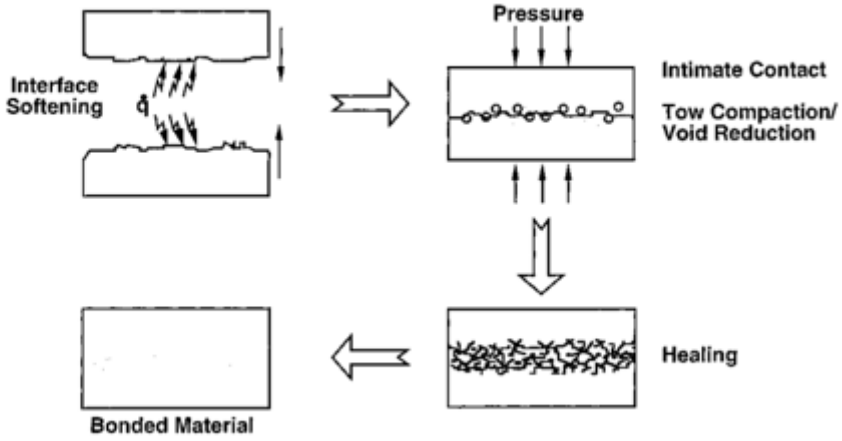


*Figure 2: Steps of the bonding process [1]*

#### *3.1.1.1 Intimate Contact Model*

The Intimate Contact Model describes the closure of the gaps between CFRP layers, thanks to an applied pressure and the viscosity of the material. It is based on the evolution of the degree of intimate contact which can be described as $D_{ic}$, the ratio of areas in contact between two layers. When $D_{ic} = 1$ , the total contact is achieved. [2] [3] Development of intimate contact depends on applied pressure, initial surface roughness and viscosity.
The viscoelastic behavior of the material is modelled as a laminar flow between two plates. For the viscosity of the bulk material the matrix-fiber mixture ($\mu_{mf}$) would have to be considered. However, if a matrix rich tape surface can be assumed its viscosity $\mu$ can be used. [4].
In order to model the initial surface roughness of CFRP Dara and Loos [5] proposed a statistical distribution of rectangles. This model was simplified by Mantell and Springer [6] using a distribution of uniform rectangles. It allows to describe the degree of intimate contact by:

$$D_{ic}(t_c) = \frac{1}{1+\frac{w_0}{b_0}}\left(1+5\left(1+\frac{w_0}{b_0}\right)\left(\frac{a_0}{b_0}\right)^2\int_0^{t_c}\frac{P_{app}}{\mu_{mf}(T)}\,dt\right)^{\frac{1}{5}}$$

where $P_{app}$ is the applied pressure, $\mu_{mf}$ is the viscosity of the matrix-fibre mixture, and $a_0, b_0, w_0$ are parameters describing the geometry of the roughness (Figure 3).

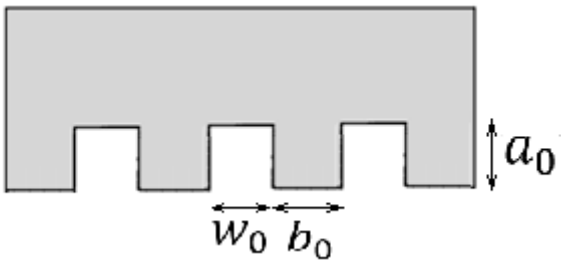


*Figure 3: Uniform Rectangles Distribution*

To better represent the intrinsic multiscale of the surface geometry, a more consistent modelling of the roughness has been proposed by Yang and Pitchumani [2]. After studying the power spectrum of profilometric data, they suggested that the surface can be modelled by a Cantor fractal description. During the AFP process, the different generations of this fractal description will be flattened one after the other, and each one is described by a degree of intimate contact $D_{ic}^{n}$:

$$D_{ic}^{n}(t_c) = \frac{1}{f^n}\left(1 + \frac{5}{4}\frac{\left(f^{\frac{2nD}{2-D}+n+4}\right)}{(f+1)^2}\left(\frac{h_0}{L_0}\right)^2 \int_0^{t_c} \frac{P_{app}}{\mu_{mf}(T)}\, dt\right)^{\frac{1}{5}}, t_{n+1} \le t \le t_n$$

where f is a scaling function, $h_0$ is the height of the first-generation asperities, $L_0$ is the total length and D is the fractal dimension of the Cantor set surface used to define the fractal model (Figure 4). The times $t_{n+1}$ and $t_n$ correspond to the starting and final times of the nth generation respectively. They can be computed with the following equation:

$$\frac{L_0}{N}\int_{t_n}^{t_{n+1}} \frac{P_{app}}{\mu_{mf}(T)}\, dt = \frac{4\left(a_{n,0}b_{n,0}\right)^3}{5}\left(\frac{1}{a_n^5} - \frac{1}{a_{n,0}^5}\right), t_{n+1} \le t \le t_n$$

where $a_{n,0}$ is the initial height of nth generation asperity, $b_{n,0}$ is the initial width, and $a_n$ is the height of nth generation asperity at time t.

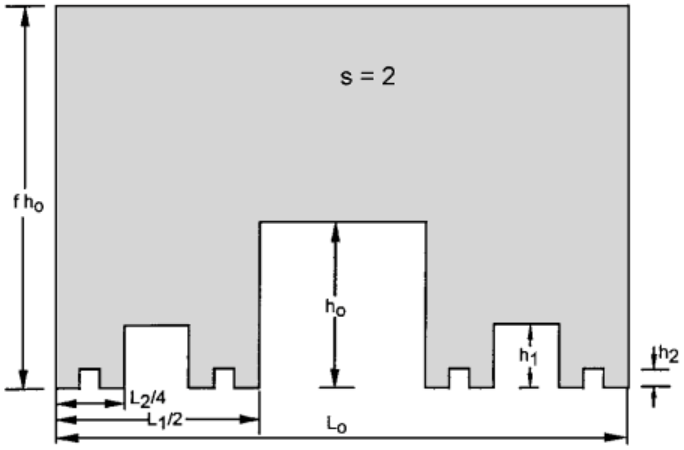


*Figure 4: Example of a Cantor set fractal surfaces [2]*

Both Mantell and Yang models were used in literature to simulate the AFP process [4] [7] [8]. In this study, both will be implemented and compared.

#### *3.1.1.2 Self-autohesion*

The self-autohesion, or healing, describes the inter-diffusion of polymer chains between two thermoplastic layers. It rests on the reptation theory of De Gennes [9]. This phenomenon can occur only when the layers are in contact and heated with a temperature above $T_m$ (melting temperature) for semi-crystalline thermoplastics. Stokes also showed that the healing may continue below $T_m$ after the melting of the polymer [7]. Self-autohesion creates bonding between the plies, and the interface disappears.
Like the intimate contact process, the healing can be described by a degree of self-autohesion $D_{ah}$. This variable is the ratio of the interfacial bond strength and the ultimate bond strength. The latter is obtained after a time called welding time.
De Gennes developed the equations for isothermal processes and they were extended to non-isothermal conditions by Yang and Pitchumani [1]:

$$D_{ah}(t_h) = \left( \int_0^{t_h} \frac{1}{t_w(T)}\, dt \right)^{\frac{1}{4}}$$

where the welding time $t_w$ decreases with the temperature. This evolution is usually described by an Arrhenius type equation. This non-isothermal description of the autohesion process will be used in this study.

#### *3.1.1.3 Bonding Model*

The bonding of CFRP prepregs tapes is an incremental process: each zone must achieve an intimate contact ($D_{ic} = 1$) before being submitted to the healing process [10] [7]. It is characterized by the degree of bonding $D_b$, which is defined by the coupling of the introduced intimate contact and self-autohesion models:

$$D_b(t_b) = D_{ic}(0) D_{ah}(t_b) + \int_0^{t_b} D_{ah}[t, t_b] \frac{dD_{ic}}{dt} dt$$

The degree of self-autohesion between times $t_1$ and $t_2$, $D_{ah}[t_1, t_2]$, defines the diffusion of polymer chains in a zone where intimate contact was only obtained for $t = t_1$. It is expressed by:

$$D_{ah}[t_1, t_2] = \left( \int_{t_1}^{t_2} \frac{1}{t_w(T)}\, dt \right)^{\frac{1}{4}} = \left( D_{ah}(t_2)^4 - D_{ah}(t_1)^4 \right)^{\frac{1}{4}}$$

When the time required to achieve intimate contact of the plies is much larger than the autohesion time, this equation can be simplified by taking $D_b = D_{ic}$ [8] [7]. The opposite phenomena could also be observed, as the residence time of the tapes under the roller, which is the available time for intimate contact to develop, is small compared to the time available for healing. In this case, some simplifications of the degree of bonding formula have been proposed [11] [12] . In this study, we will use the general expression of the degree of bonding as the characteristic times of the two mechanisms that were obtained with the models are close.

### *3.1.2 Experimental*

In order to use introduced models, specific material characteristics have to be determined: roughness parameters, viscosity and weld time. The first is yielded by profilometry following the presented models. [2] [4]. The viscosity and the welding time will be measured with a rheometer, using Bonmatin data and procedure [13]. For all trials a CF/LM-PAEK with a fiber volume fraction of 66% supplied by Toray was used. When needed, neat polymer of the same chemical composition as the matrix (grade AE250, supplied by Victrex) was used.. The experiments and results are discussed in the following section.

#### *3.1.2.1 Profilometry trials*

The trials were performed with a VK-X1000 Keyence laser scanning microscope on the unprocessed prepreg tape. In order to remove the bending of the tape, two aluminum weights were used (see Figure 5). For the model of Yang and Pitchumani the measured profile needs to have a total length $L_p = 1/f_{min}$ where $f_{min}$ will be the minimal frequency of the power spectrum. It is computed via Fast Fourier Transformation (FFT). Moreover, the profile must have an accuracy $\Delta x = 1/4f_{max}$ where $f_{max}$ is the maximal frequency of the power spectrum. This results in a measured profile length of $L_p = 1.8mm$ and with an accuracy of $\Delta x = 0.7\ \mu m$.

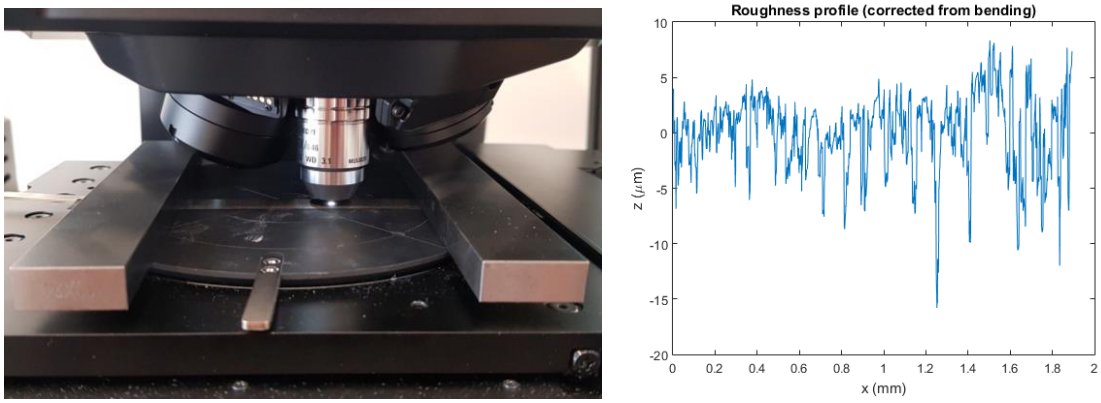


*Figure 5: Profilometer set up and Toray roughness profile*

The obtained results can also be fed into the model of Mantell and Springer, using the statistical methods described by Schaefer [4]. Parameter $L_0$ is determined by the inverse of the frequency corresponding to the lower boundary of the linear range. It should be representative of the largest repeating unit, and was fixed at 0.3mm after studying power spectrums. Other parameters were also calculated following Yang [2] and Schaefer [4] recommendations. The results of these profilometry trials are presented in Table 1:

*Table 1: Parameters Intimate contact model for CF/LM-PAEK*

| Model | Parameter | Value (mean) | Error |
|---|---|---|---|
| **Yang&Pitchumani** | D | 1.55 | 3% |
| | f | 1.26 | 6% |
| | $h_0$ (μm) | 6.8 | 14% |

| | | | |
|---|---|---|---|
| | $L_0$ (mm) | 0.3 | |
| **Mantell&Springer** | $a_0$ (µm) | 6.8 | 14% |
| | $b_0$ (µm) | 22 | 12% |
| | $w_0$ $(\mu m)$ | 38 | 11% |

The parameters of the fractal model obtained from the CF/LM-PAEK profiles are in the same order of magnitude than those obtained for carbon fiber reinforced PEEK. [2] [8]. In particular, parameters $h_0$ and $a_0$ are close to the diameter of a single carbon fiber, which validates this result. Besides, the number of asperities on a repeating segment of the Cantor set block $s$ can be calculated from the parameters $D$ and $f$ from the following formula:

$$s = f^{\frac{D}{2-D}}$$

With the parameters given in Table 1, $s = 2.2$. This is a consistent value as it is close to an integer value of 2 which gives a physical meaning to the Fractal model.

The parameters of the Mantell and Springer models were also validated by comparing the ratio $a_0/b_0$ and $w_0/b_0$ with literature data on PEEK [14].

*3.1.2.2 Rheological trials*

In order to implement the bonding, the viscosity and welding time of LM-PAEK need to be measured for typical process temperatures: between 305 and 350°C. Bonmatin characterized these rheological parameters for LM-PAEK in a recent article. These values are extended for lower temperatures following the same method. [13]

The rheological characterization is conducted with a MCR302 Anton Paar rheometer using the neat matrix AE250 supplied by Vitrex as we consider the interface of the composite tape to have a thin polymer layer. This hypothesis was also used by Tierney and Schaefer [11] [4]. A plate-plate (25mm) configuration was used and a frequency sweep applied with a shear deformation of 0.5% to stay in the linear range but still have good precision in the measurements. As a thicker material was not available, 100µm thick films were used. The parallelism of the plates needed to account for such thin samples was achieved by using adapted plates supplied by Anton Paar.

To ensure a complete melting a temperature of 320°C was used. The degradation at high temperatures (cross-linking), noted by Bonmatin, was also observed in our trials. For example, an increase of the viscosity by 10% was measured during a 15 minutes study at 350°C. The samples were therefore changed at each trial for a better accuracy.
The zero-shear-rate viscosity obtained on our samples are close to the ones obtained by Bonmatin (see Figure 6, black and blue dots respectively), even if the deviation in the data stays important because of the difficulty to control cross-linking (around 35% at 350°C). They are also validated by the TTS given in her study [13]. An Arrhenius fit of the form $A \exp\left(-\frac{E_a}{RT}\right)$ is realized on the data. The values of the parameters are summarized in Table 2.

*Table 2: Parameters of the Viscosity model (Arrhenius)*

| | |
|---|---|
| $A$ **- Arrhenius Constant [Pa.s]** | 6.2e-3 |
| $E_a$ **- Activation Energy [J/mol]** | 6.6e4 |

The neat LM-PAEK has a lower viscosity than PEEK which will facilitate the intimate contact mechanism. For the matrix-fiber mixture a higher viscosity can be expected, this is depicted by the values of Khan (see Figure 6, violet solid line).

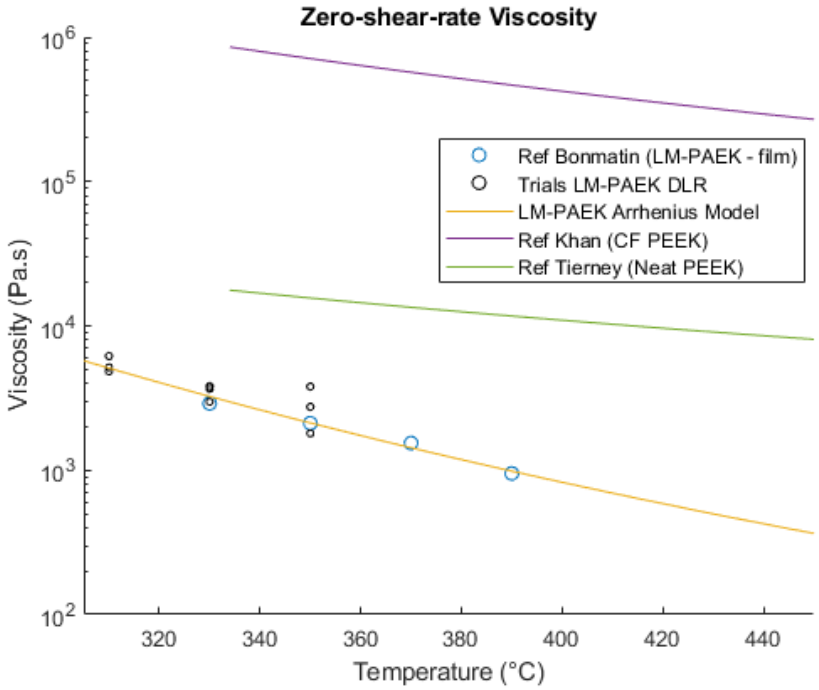


*Figure 6: Comparison of the LM-PAEK and PEEK viscosity models [13] [8] [11]*

One can measure two relaxation times: $\tau_n$ associated with the motion of the shortest chains, and $\tau_w$ describing the motion of the longest chains in quasi-static and long processes. The welding time can be approximated by the longest time $\tau_w$ for fast processes during which cross-linking is negligible [15]. The relaxation times obtained through rheological measurements are higher than those obtained by Bonmatin (around twice the time at 330°C). It could be explained by the uncertainty of the method employed to compute the time $t_w$, but also by cross-linking effects. Confinement effects due to the thin films could also have an impact on the diffusion of the polymer chains. But those effects would also appear during AFP as only a thin polymer layer is present at the interface.

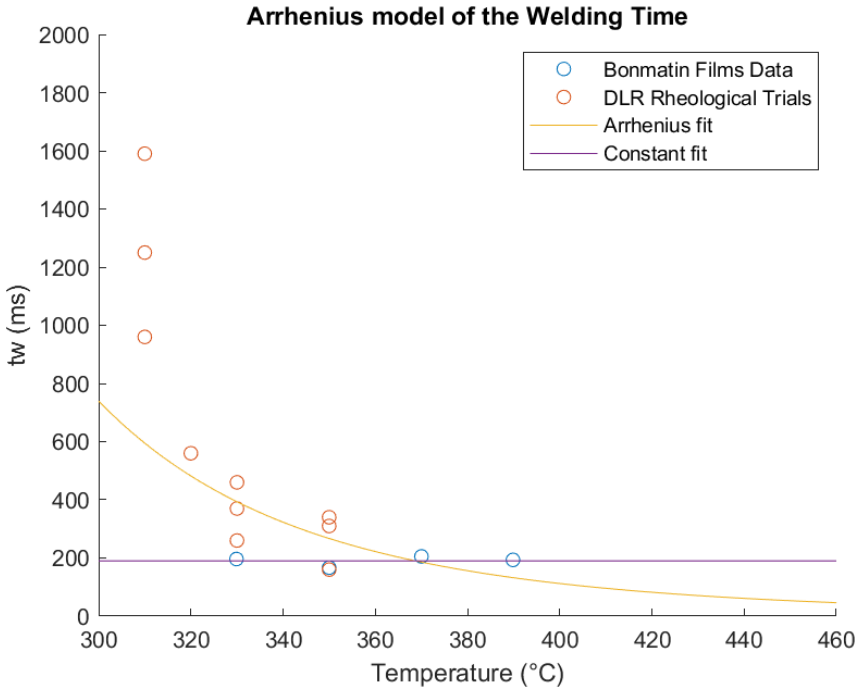


*Figure 7: Fitting of an Arrhenius model on the welding times data*

When considering Bonmatin values, the welding time $\tau_w$ seems to be constant in the temperature range of 330 - 390°C. As first approximation, it can be modeled by a constant value, equal to 190ms above 305°C. This model would respect the order of magnitude of the welding time, but could lead to underestimate the healing time.

In our data, we can observe a tendency that is closer to the one predicted in literature, with an increase of the welding time for lower temperatures. Even if the deviation is important, we can fit an Arrhenius model on them (see Figure 7). Parameters are given in Table 3.

*Table 3: Parameters of the Welding time Arrhenius model*

| | |
|---|---|
| **$A$ - Arrhenius Constant [s]** | 2.3e-6 |
| **$E_a$ - Activation Energy [J/mol]** | 6.0e4 |

### *3.1.3 Implementation*

The intimate contact, healing and bonding models are numerically implemented with MATLAB using the determined parameters. As the viscosity and weld time are considered as infinite under $T_m$ to decouple bonding and crystallinity models. Required inputs for the bonding models are consolidation pressure and material temperature gradients. The first is constant at 6 bars and the latter is retrieved from an existing heat transfer simulation.

## 3.2 Crystallization Models

### *3.2.1 State of the art and Models selection*

The final morphology of the semi crystalline thermoplastic matrix (linked to the degree of crystallinity, spherulite sizes or crystalline orientation) will affect the mechanical and thermal properties of the CFRP material. Crystallinity is mainly dependent on the temperature history. If the temperature is below the glass transition temperature $T_g$, the crystallization state will be fixed. If the temperature is above the melting temperature $T_m$, the crystallites will melt until reaching an amorphous state and between $T_g$ and $T_m$, the crystallites will grow.

In order to describe these different phenomena, two models are needed: a growth model and a melting model. They need to describe the highly non-isothermal TP-AFP process with high heating and cooling rates.

#### *3.2.1.1 Crystallization growth models*

During crystallization growth two mechanisms occur: primary crystallization describes the spontaneous growth of crystallites from the melted material or fibers. This kinetic can be quite fast, as it occurs with higher cooling rate than 400°C/min. The secondary crystallization describes the development of spherulites from the previously formed crystallites [16].

Crystallites growth models are mostly based on Avrami or Tobin equations. The first method has shown good efficiency in modelling non-isothermal conditions. The Avrami equation under non-isothermal conditions can describe the evolution of one crystallization mechanism. The degree of crystallinity $X_{vc}$ evolves between 0 and $X_{vc,\infty}$, the equilibrium volume fraction of crystallinity. The kinetic is modelled thanks to two parameters: $n$, which represents the type of growth (equal to 3 for 3D spherulites instantaneous growth, for the primary crystallization) and $K$, the temperature dependent crystallization rate.

$$\frac{X_{vc}(t_c)}{X_{vc,\infty}} = 1 - \exp\left(-\int_0^{t_c} K(T) n t^{n-1} dt\right)$$

Secondary crystallization will play a minor role due to the transient nature of TP-AFP. By neglecting this phenomenon, the kinetic of crystallization can be modelled by a simple Avrami equation. Else, more complex models would be needed like the Velisaris and Seferis model [17].

#### *3.2.1.2 Crystallites melting model*

Crystallites melting can be described by the Maffezzoli model. This model could be fitted by studying melting enthalpy in DSC studies involving high heating rates. But, as a first approximation, it was chosen to consider a complete melting of the LM-PAEK material at the interface of the tapes during AFP. This complete melt is necessary to observe a bonding between the layers.

### *3.2.2 Experimental*

In order to model the crystallization growth, the Avrami parameters have to be characterized. This could not be achieved with a standard Differential Scanning Calorimeter, NETZSCH DSC

214 Polyma. Indeed, this device is limited to cooling rates of 500K/min and need a typical time of 1 minute to stabilize at a chosen temperature. So, the kinetic of crystallization of LM-PAEK was hidden when trying to study isothermal steps, even when employing Choupin's post-processing method [18].

To access fast crystallization kinetic, trials can be realized in a Mettler Toledo Flash DSC 2+. As the samples dimension must be very small in such a device (diameter around 150 µm), 100µm-thick neat AE250 was used.

#### *3.2.2.1 Crystallization growth analysis*

The Avrami equation can be fitted from half-times of crystallization measurements given by Victrex, through the following equation:

$$\tau^{\frac{1}{2}} = \left(-\frac{\ln(0.5)}{K}\right)^{\frac{1}{n}}$$

These half-times of crystallization were measured on isothermal steps at different temperatures, after a complete melting of the polymer. They will be representative of the hot crystallization growth,

An Avrami equation was fitted on the data by considering a gaussian evolution, for the growth factor K:

$$K(T) = A \exp\left(-\frac{(T - T_c)^2}{\sigma_T^2}\right)$$

This function has an evolution which is close to the one predicted by the models developed in Hoffmann and Lauritzen theory. But its parameters are easier to fit as they have a physical meaning: $T_c$ is the temperature at which crystals grow the fastest, $\sigma_T$ characterizes the range of temperatures in which crystallization can develop and $A$ is the factor which quantifies the growth velocity. The Avrami parameter $n$ was chosen to be 3 as the primary crystallization is characterized by a 3D evolution of spherulites.

The results of the Gaussian modelling are presented in Figure 8 and Table 4.

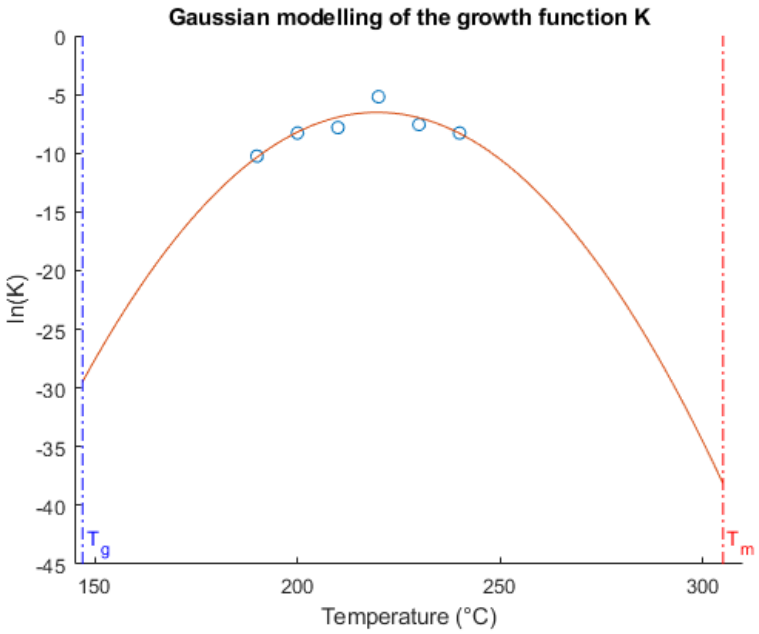


*Figure 8: Fitting of a Gaussian model on the growth factor K data obtained from flash DSC studies*

*Table 4:Parameters of the Avrami growing factor Gaussian model*

| | |
|---|---|
| **$A$ - Arrhenius Constant [$s^{-3}$]** | 1.5e-2 |
| **$T_c$ – Crystallization Temperature [°C]** | 220 |
| **$\sigma_T$ – Temperature deviation [°C]** | 15 |

Besides, secondary crystallization could not be accurately observed on the resulting heat flux curves from isothermal studies. Optimizing the Velisaris and Seferis model on the data resulted in a negligible growing function $K_2$ of the secondary crystallization, in front of the growth function of primary crystallization $K_1$. The estimation of $K_2$ was therefore judged not accurate enough to predict secondary crystallization. But as the process durations are quite short in AFP, this slow phenomenon should not have a crucial impact.

### *3.2.3 Implementation*

The Avrami equation was implemented following the numerical scheme proposed by Choupin [18]. No coupling is necessary between the melting and growth models. A simple threshold at 305°C allows to choose between the two models when computing the crystallization kinetic. The only input required by the crystallization model is the temperature gradient as pressure effects are supposed negligible.

## 3.3 Coupling of the Bonding and Crystallization models

In theory, the bonding and crystallization models need a coupling as they can interact with each other. Due to the fact that the crystallization process slows down the migration of the polymer chains by modifying the relaxation time of the LM-PAEK. As mentioned earlier in this study it is assumed that the bonding process is stopped when going below the melting temperature.

With this hypothesis, the bonding and the crystallization are consecutive processes and no coupling is needed (refer to Figure 9).

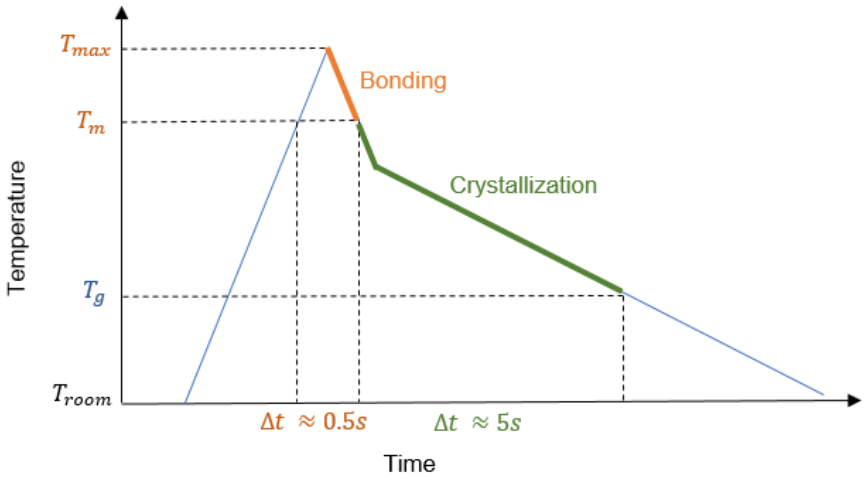


*Figure 9: Bonding and Crystallization processes in AFP, for a typical temperature curve*

# 4. VALIDATION

## 4.1 Bonding Model Validation

### *4.1.1 Mechanical Testing*

The bond strength $\sigma$ of the interface, developed during AFP, has to be measured to validate the bonding model presented above. This is usually done by Interlaminar Shear Strength Tests (ILSS) like short beam strength trials or Double Cantilever Beam trials. [7] [11] [8]

For this study perpendicular tensile testing following the standard DIN EN 2564 was performed. The layup velocity and laser power were varied to manufacture samples with different AFP conditions. Tests were carried out on a universal ZwickRoell 50 kN testing machine. A reference, created in hot press to achieve the ultimate bonding strength $\sigma_\infty$, was also used to compute the experimental final degree of bonding $D_b = \sigma/\sigma_\infty$.

ILSS trials were first done on these specimens but the failure mode did not correspond to the norm because of the ductile behavior of thermoplastics. It was therefore chosen to use perpendicular tensile tests to measure the interface strength.

### *4.1.2 Comparison trials and bonding models' predictions*

Final degree of bonding was predicted with different models: Fractal and Uniform Rectangles Models of the intimate contact, and Constant or Arrhenius models of the welding time. Different roller velocities, of 125, 250 and 400 mm/s were used. Laser powers, allowing to reach correct processing temperatures were chosen for each velocity. Besides, different laser powers of 2300, 2450 and 2600W were tried for a velocity of 125mm/s, typically used with the laser AFP setup. For each velocity and pressure pair, the corresponding pressure and temperature histories were obtained with Fujifilms and thermocouples studies. Results are presented in Figure 10 and Figure 11.

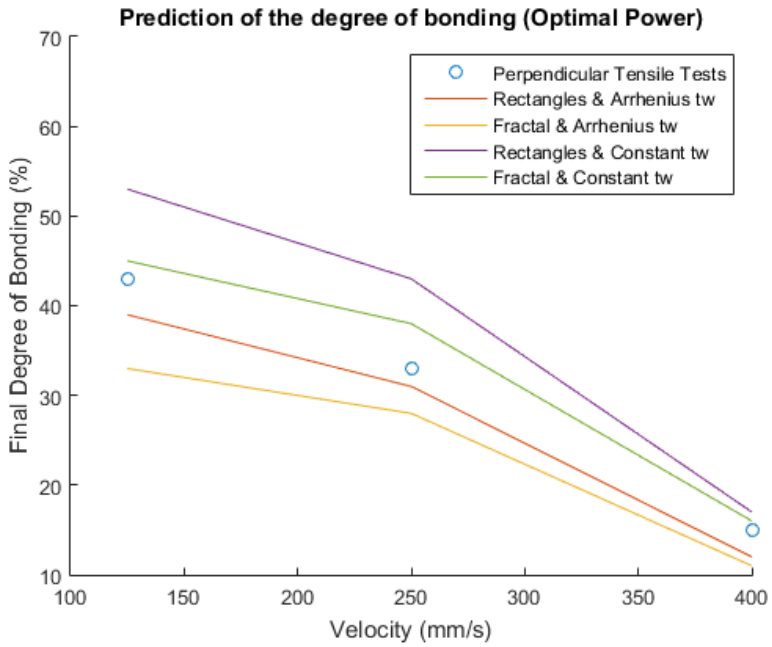


*Figure 10: Prediction of the bonding and comparison with Perpendicular Tensile Tests data - for roller velocities of 125, 250 and 400 mm/s*

From these figures, the most promising model seem to be the one coupling a fractal description of surface roughness, and a constant approximation of the welding time (green line in Figure 10 and Figure 11). An error of prediction of only 15 % is measured with the AFP conditions used.

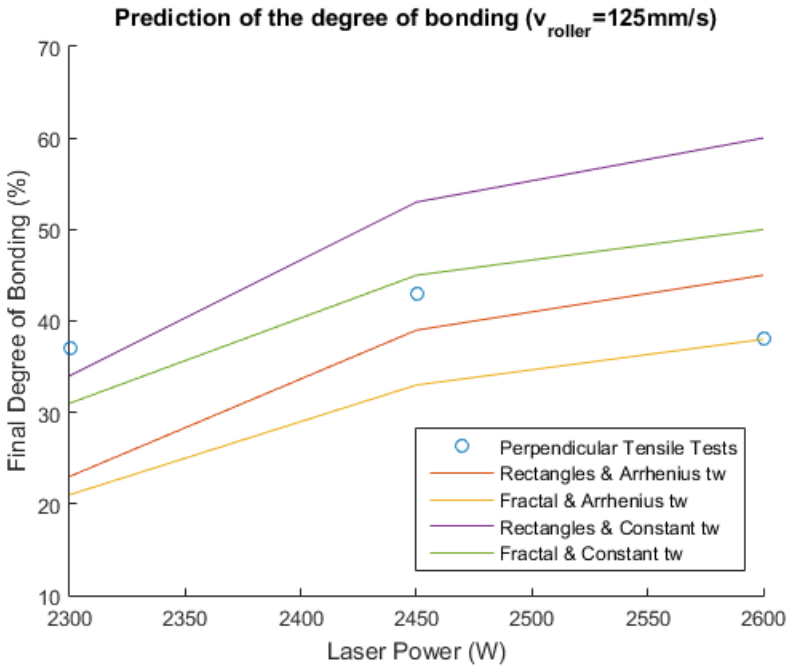


*Figure 11: Prediction of the bonding and comparison with Perpendicular Tensile Tests data - for laser powers of 2300, 2450 and 2600 W*

The model describing the surface roughness with a rectangle distribution, and the welding time by an Arrhenius evolution (red line in Figure 10 and Figure 11) also provides good results with

a mean error of also 15%. But the degree of bonding for a laser power of 2300W and a velocity of 125mm/s is rather underestimated. This result could be due to the fact that with these conditions, the processing temperatures are closer to the melting temperature. The short process window could prevent the longer chains to have a major impact on the interface strengthening, and the bonding could therefore be mainly provided by shorter chains which have a faster diffusion time. In that case, the final degree of bonding predicted would be higher than the one computed with our hypothesis on the welding time.

The other models presented in Figure 10 and Figure 11 tend to overestimate or underestimate the degree of bonding of AFP-manufactured parts. But more validation data will be generated in future studies to validate these first predictions.

None of the models describes the drop of interface bonding for a velocity of 125 mm/s and power of 2600 W. The bad mechanical performance could be explained by a temperature after the passing of the roller that was still greater than the melting temperature. In these conditions, the thermoplastic matrix could flow freely as no pressure was applied anymore. Therefore, deconsolidation could have been obtained. This phenomenon should also be added to our bonding model.

## 4.2 Crystallization Model Validation

### *4.2.1 DSC trials*

To validate the models, the crystallization literature values were used. These were obtained on a Netzsch DSC214 Polyma device, with a temperature range of −40°C to 600°C and maximum heating/cooling rate of 500°C/min. Trials were realized on AFP-manufactured samples to measure the final degree of crystallinity of the CF/LM-PAEK. [16]

### *4.2.2 Comparison trials and crystallization models' predictions*

In their study, Raps et al. measured a crystallinity after the AFP process with a 20 °C tool that was very close to the initial value, between 7.5 % and 9.0 %. This value was calculated for four layers samples, manufactured with AFP. To predict the final degree of crystallization with our models, the temperature input was taken from thermocouples study of the placement of three layers above a fourth one, with a layup speed of 7.5 mm/s (velocity used by Raps).

The Avrami model presented above predicted a degree of crystallization of 5.7 % under those temperature conditions (see Figure 12). This first result shows that crystallization on a specific point should mainly occur when several layers are placed above it with AFP. It means that cold crystallization should be the main process involved in the growth of the crystallites. Besides, an important inhomogeneity could be the result in AFP-manufactured parts.

The discrepancy between our result and the final degree of crystallinity measured by Raps could have several explanations. Indeed, hot and cold crystallization have different kinetic that were not differentiated in our models. The degree of crystallinity was also measured on the whole specimens, even if it is probably not homogeneous throughout the thickness. Moreover, it could be possible that only the interface of the tape is heated and melts during AFP, because of the carbon fibers. This would lead to a conservation of the initial degree of crystallization inside each layer, in most of the thickness. Finally, the Avrami model is a very simple one

which do not consider secondary crystallization or the impact of the fibers and crystallites themselves on the crystallization kinetic.

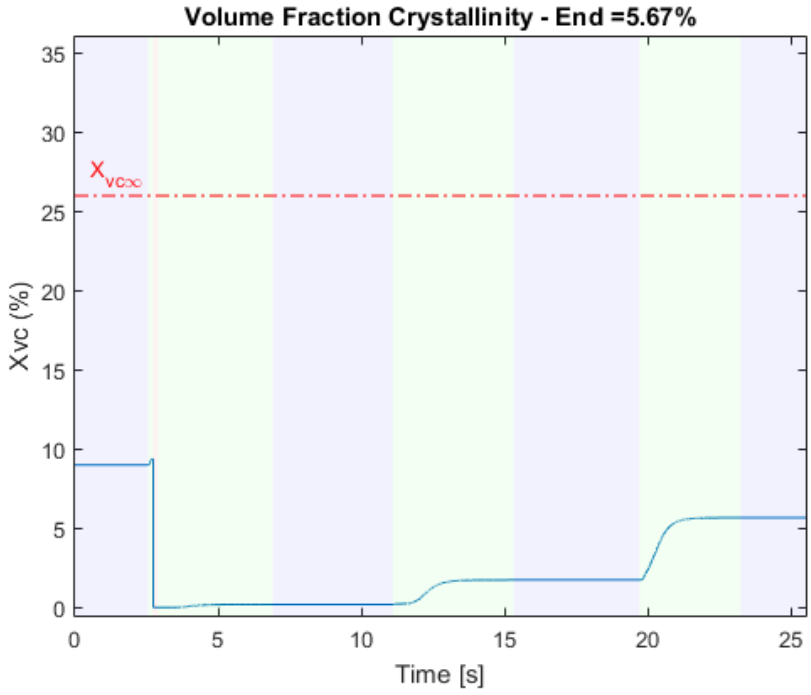


*Figure 12: Crystallization kinetic during the placement of 3 layers, at the first layer interface*

## 5. DISCUSSION AND CONCLUSION

This study has presented a methodology to implement, optimize and validate bonding and crystallization models for a fast process such as the Automated Fiber Placement. This method is interesting as it allows to better understand the crucial physical phenomena involved in AFP, while reducing the number of trials and the quantity of material needed to master the end-of-process quality.

The models presented could predict the bonding and crystallization kinetic during AFP, using temperature, speed and pressure as inputs. In particular, the bonding model involving a Fractal representation of the tapes' roughness and a constant approximation of the welding time showed good predictions with an error of approximatly 15 %. The crystallization model showed that cold crystallization should be the main growth mechanism to explain the final degree of crystallinity. More validation data should be generated to better optimize the models on CF/LM-PAEK, in particular for rheological and crystallization trials.

Modelling fast manufacturing processes involve several challenges. A multi-physics approach, with models coupling, need to be adopted. Adapted devices must also be used to characterize the material in representative conditions.

This work also highlighted some specific phenomena that should be studied more thoroughly. The polymer chains diffusion in a polydisperse thermoplastic, and their participation in the strengthening of the bonded interface is still not well understood. Furthermore, the thickness

of the tape that is heated and melted by the laser should be accurately measured. Indeed, only in this region will the crystallinity evolve. This polymer thickness will also be the only one to participate in the bonding process.

Linked to a thermal finite element simulation of AFP, these models could also be used to predict the best processing parameters. Indeed, the FEM could give the temperature and pressure history in the material from AFP parameters inputs that could be used for quality prediction model. Thus, processing maps of the AFP process could be drawn. Additionally degradation models could also be coupled to these models to avoid selecting adverse parameters resulting in too high temperatures.

Finally, this methodology could also be applied to other materials, close to the Low-Melt PAEK reinforced with carbon fibers, that was used here. The models would also be useful to predict quality after other processes like hot press forming or welding. In those cases, the difference in the duration of the process could allow to simplify the models, by neglecting the healing process for example.

## 6. ACKNOWLEDGMENT

This project has received funding from the Clean Aviation Joint Undertaking (CAJU) under grant agreement CS2-LPA-GAM-2020-2023-01. The JU receives support from the European Union's Horizon 2020 research and innovation programme.

We would like to thank VICTREX, especially Mr. Frank Schemm, for providing the resin films for our investigations and his great support on gathering and sharing valuable data on LM-PAEK. We are also grateful for the support of the University of Augsburg, and in particular to Mr. Tobias Karrasch and Mr. Robert Horny, for supplying experimental devices and for their support during testing. Lastly, we would like to extend our sincere thanks to Mrs. France Chabert for providing expertise on thermoplastics rheology.

## 7. DISCLAIMER

The results, opinions, conclusions, etc. presented in this work are those of the author(s) only and do not necessarily represent the position of the CAJU; the CAJU is not responsible for any use made of the information contained herein.

## 8. REFERENCES

[1] F. Yang and R. Pitchumani, "Healing of Thermoplastic Polymers at an Interface under Nonisothermal Conditions," *Macromolecules,* vol. 35, pp. 3213-3224, 2002.

[2] F. Yang and R. Pitchumani, "A fractal Cantor set based description of interlaminar contact evolution during thermoplastic composites processing," *Journal of Materials Science,* vol. 36, p. 4661–4671, 2001.

[3] F. O. Sonmez and H. T. Hahn, "Modeling of heat Transfer and Crystallization in Thermoplastic Composite Tape Placement Process," *Sonmez, Fazil O. and Hahn, H. Thomas*, 1997.

[4] Schaefer, T. Guglhoer, M. Sause and K. Drechsler, "Development of intimate contact during processing of carbon fiber reinforced Polyamide-6 tapes," *Journal of Reinforced Plastics and Composites*, vol. 36, pp. 593-607, 2017.

[5] A. Dara and P. Loos, "Thermoplastic matrix composite processing model," Virginia Polytechnic Institute and State University, 1985.

[6] S. C. M. Springer and G. S., "Manufacturing Process Models for Thermoplastic Composites," *Journal of Composite Materials*, vol. 26, pp. 2348-2377, 1992.

[7] C. Stokes-Griffin and P. Compston, "Investigation of sub-melt temperature bonding of carbon-fibre/PEEK in an automated laser tape placement process," *Composites Part A: Applied Science and Manufacturing*, vol. 84, pp. 17-25, 2016.

[8] M. A. Khan, P. Mitschang and R. Schledjewski, "Identification of some optimal parameters to achieve higher laminate quality through tape placement process," *Advances in Polymer Technology*, vol. 29, pp. 98-111, 2010.

[9] P. De Gennes, "Reptation of a Polymer Chain in the Presence of Fixed Obstacles," *The Journal of Chemical Physics*, vol. 55, pp. 572-579, 1971.

[10] F. Yang and R. Pitchumani, "Nonisothermal Healing and Interlaminar Bond Strength Evolution During Thermoplastic Matrix Composites Processing," *Polymer Composites*, vol. 24, pp. 263 - 278, 2003.

[11] J. Tierney and J. W. J. Gillespie, "Modeling of In Situ Strength Development for the Thermoplastic Composite Tow Placement Process," *Journal of Composite Materials*, vol. 40, pp. 1487-1506, 2006.

[12] R. Pitchumani, S. Ranganathan, R. Don, J. Gillespie and M. Lamontia, "Analysis of transport phenomena governing interfacial bonding and void dynamics during thermoplastic tow-placement," *International Journal of Heat and Mass Transfer*, vol. 39, pp. 1883-1897, 1996.

[13] M. Bonmatin, F. Chabert, G. Bernhart and T. Djilali, "Rheological and crystallization behaviors of low processing temperature poly(aryl ether ketone)," *Journal of Applied Polymer Science*, vol. 138, p. 51402, 2021.

[14] O. Çelik, D. Peeters, C. Dransfeld and J. Teuwen, "Intimate contact development during laser assisted fiber placement: Microstructure and effect of process parameters," *Composites Part A: Applied Science and Manufacturing*, vol. 134, p. 105888, 2020.

[15] J. Avenet, T. A. Cender, S. Le Corre, J.-L. Bailleul and A. Lévy, "Experimental correlation of rheological relaxation and interface healing times in welding thermoplastic PEKK composites," *Composites Part A: Applied Science and Manufacturing*, vol. 149, 2021.

[16] L. Raps, A. Chadwick, I. Schiel and I. Schmidt, "CF/LM-PAEK: Characterisation and sensitivity to critical process parameters for automated fibre placement," *Composite Structures*, vol. 284, p. 115087, 2022.

[17] C. N. Velisaris and J. C. Seferis, "Crystallization kinetics of polyetheretherketone (peek) matrices," *Polymer Engineering & Science*, vol. 26, pp. 1574-1581, 1986.

[18] T. Choupin, "Thesis: Mechanical performances of PEKK thermoplastic composites linked to their processing parameters," 2017.

[19] Y. D. Boon, S. C. Joshi and S. K. Bhudolia, "Review: Filament Winding and Automated Fiber Placement with In Situ Consolidation for Fiber Reinforced Thermoplastic Polymer Composites," *Polymers,* 2021.

[20] Z. Kou, J. Xiao, D. Huan, K. Zhu and L. Yan, "Optimization of thermal model and prediction of crystallinity during the laser-assisted tape winding process," *Journal of Reinforced Plastics and Composites,* vol. 40, pp. 606-618, 2021.

[21] A. Maffezzoli, K. JM. and L. Nicolais, "Welding of PEEK/carbon fiber composite laminates," *SAMPE J,* vol. 25, pp. 35-39, 1989.

[22] J. Tierney and J. Gillespie, "Crystallization kinetics behavior of PEEK based composites exposed to high heating and cooling rates," *Composites Part A: Applied Science and Manufacturing,* vol. 35, pp. 547-558, 2004.